

Recent Electroweak Results from the Tevatron

Krishnaswamy Gounder

University of California, Riverside, CA 92521, USA.

(For the CDF and DØ Collaborations)

Recent electroweak results from the CDF and DØ Collaborations at the Fermilab Tevatron Collider are presented. After a brief description of the DØ measurements of W/Z production cross sections, W width, W mass and $W \rightarrow \tau\nu$ decays, the CDF result on $W(p_T)$ distribution is outlined. The comprehensive search for anomalous gauge couplings by DØ in 1992-96 data is presented along with a detailed description of the $WW/WZ \rightarrow \mu\nu jj$ channel.

I. INTRODUCTION

The CDF [1] and DØ [2] collaborations at the Fermilab Tevatron collider collected data during Run I (1992-96) at $\sqrt{s} = 1.8$ TeV corresponding to an integrated luminosity of about 130 pb^{-1} for each experiment. The large number of W and Z bosons detected in the electron and muon channels were used to make precise measurements of their properties. The $W \rightarrow \tau\nu$ decay was studied by both experiment to measure the ratio g_τ^W/g_e^W . Using the Run I data, DØ has made a comprehensive search for anomalous trilinear gauge couplings in 12 different diboson channels and has combined them to produce some of the most stringent anomalous gauge coupling limits in the world so far.

Run I was divided into three different sections: Run 1A - 1992-93 ($\sim 20 \text{ pb}^{-1}$); Run 1B - 1993-95 ($\sim 90 \text{ pb}^{-1}$); Run 1C - 1995-96 ($\sim 20 \text{ pb}^{-1}$). After a brief review of W and Z properties in Section II, the DØ search for anomalous gauge couplings in the diboson final states is presented in Section III.

II. ELECTROWEAK MEASUREMENTS

A. W and Z Boson Production

Due to cleaner signatures and lower backgrounds, the W and Z bosons are detected via their leptonic decays: $W \rightarrow e\nu, \mu\nu$ and $Z \rightarrow ee, \mu\mu$. The W event selection requires an electron (muon) with $p_T > 25$ (20) GeV/c and $\cancel{E}_T > 25$ (20) GeV in the event. For Z selection, the \cancel{E}_T requirement is replaced by that of a similar second lepton. The backgrounds for the W electron sample are mainly due to QCD fakes (5.7%), τ decays (1.8%) and one-legged Z decays (0.6%). The total background for the $W \mu$ sample is 19.8% including cosmic muons. The e and μ Z samples contain 4.8% and 11.6% backgrounds respectively with additional contributions from Drell-Yan pairs and combinatorics.

The recent W and Z cross section results from CDF and DØ are shown in Figure 1 and are compared to the $O(\alpha_s^2)$ theoretical QCD prediction [3]. When the ratio of W and Z cross sections is computed many uncertainties cancel and an indirect measurement of the W width can be made:

$$R_l = \frac{\sigma \cdot B(W \rightarrow l\nu)}{\sigma \cdot B(Z \rightarrow ll)} = \frac{\sigma(W)}{\sigma(Z)} \cdot \frac{(W \rightarrow l\nu)}{(Z \rightarrow ll)} \cdot \frac{1}{BR(Z \rightarrow ll)}$$

With the measured ratio of $R_l = 10.6 \pm 0.3$, a value of $\sigma(W) = 2.06 \pm 0.06$ is obtained from the above equation by using the a theoretical calculation of σ_W/σ_Z , the precise measurement of $B(Z \rightarrow ll)$ from LEP, and the theoretical computation of $(W \rightarrow l\nu)$. A comparison of R_l measurements is shown in Figure 1 along with the Tevatron average. An updated and expanded W/Z production results can be found in reference [4].

B. W Mass

The W boson mass is a fundamental parameter of the Standard Model. In the on shell scheme:

$$M_W = \left(\frac{\pi\alpha(M_Z^2)}{\sqrt{2}G_F} \right)^{1/2} \frac{1}{\sin\theta_W\sqrt{1-\Delta r}}$$

where M_Z is the Z boson mass, α is the fine structure constant, θ_W is the weak mixing angle, G_F is the Fermi coupling constant and Δr denotes the radiative corrections. The Δr is sensitive to masses of particles such as the Higgs boson, top quark and other new particles. Therefore, a precision measurement of the M_W can be used for constraining the Higgs mass or probing the presence of new physics beyond the SM [5].

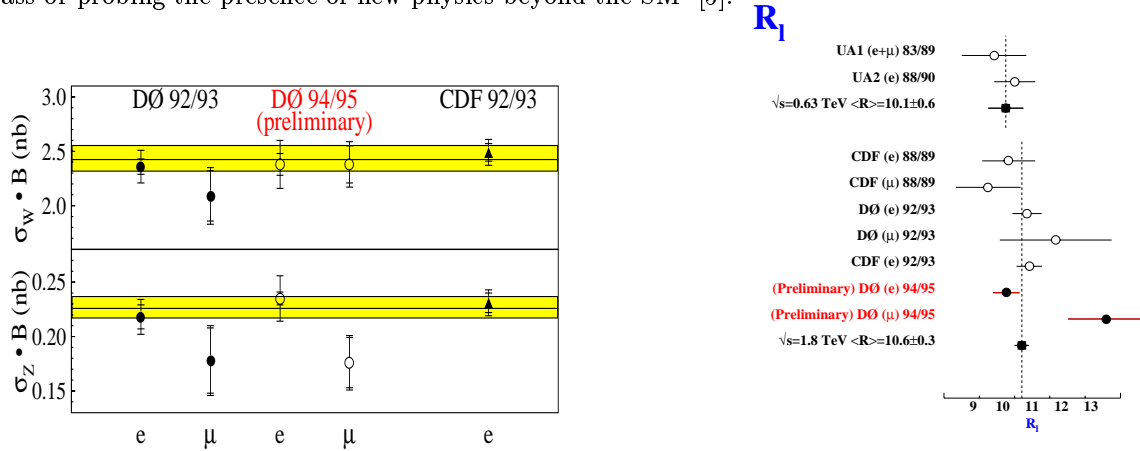


FIG. 1. The Tevatron measurements of $\sigma \cdot B$ for inclusive W and Z production are shown on the left. The shaded bands are the $O(\alpha_s^2)$ theoretical QCD predictions. On the right, a summary of R_l measurements including the Tevatron average.

The W mass is measured using the decay $W \rightarrow e\nu$ with a total luminosity of $\int \mathcal{L} dt = 80 pb^{-1}$. As an unknown amount of energy goes down the beam pipe in the forward and backward directions, the $p_L(\nu)$ remains uncertain. Hence, the W mass is determined using a likelihood fit to the transverse mass $M_T(e\nu) = [2p_T^e p_T^\nu (1 - \cos \phi^{e\nu})]^{1/2}$. A similar procedure is applied to $p_T(e)$ and $p_T(\nu)$ as cross checks.

The event selection and backgrounds are similar to the cross section measurement. Event selection with a high quality isolated electron in the central region with $p_T(e) > 25$ GeV/c, $\cancel{E}_T > 25$ GeV and hadronic recoil < 15 -20 GeV/c leads to a final sample of about 28,000 events. The $p_T(\nu)$ depends on the recoil momentum of the electron and hadrons which relies on the detailed understanding and modelling of the leptonic and hadronic energy scales. The DØ electromagnetic energy scale was calibrated using the constraints from decays $Z \rightarrow ee$, $J/\psi \rightarrow ee$ and $\pi^0 \rightarrow \gamma\gamma$ as shown in Figure 2 where α and δ are given by $E_{meas} = \alpha E_{true} + \delta$. A complete list of uncertainties contributing to the W mass measurement is listed in Table I.

The fit to the $M_T(e\nu)$ distribution is shown in Figure 2. The arrows indicate the fitted region for the final measurement and the shaded region represents background in the sample. The results from the $M_T(e\nu)$ and $p_T(e)$ fits using the Run 1B data are $80.44 \pm 0.01 \pm 0.07$ and $80.48 \pm 0.11 \pm 0.14$ GeV/c² respectively. Combining with the 1A measurement, DØ 1A + 1B: $M_W = 80.43 \pm 0.11$ GeV/c². A summary of direct M_W measurements is shown in Figure 3 along with the world average. Figure 3 also illustrates the constraints imposed by the direct measurements of M_W and M_t by CDF and DØ on the mass of the Higgs boson. Also shown are the indirect SLC/LEP2 and NuTeV [6] measurements and the prediction of the Minimal Supersymmetric Model (MSSM). An update DØ W mass measurements including forward detectors can be found in reference [4].

TABLE I. Summary of uncertainties and their sources in the measurement of M_W using a maximum likelihood fit of $M_T(e\nu)$ and $p_T(e)$ distributions (in MeV/c²).

Source	M_T Fit	$p_T(e)$ Fit	Source	M_T Fit	$p_T(e)$ Fit
W Statistics	70	85	Electron Energy Scale	65	65
Calorimeter Linearity	20	20	Calorimeter Uniformity	10	10
Electron Energy Resolution	25	15	Electron Angle Calibration	30	30
Electron Removal	15	15	Selection Bias	5	10
Hadronic Recoil Modelling	30	20	Input $p_T(W)$ and PDF's	25	70
Radiative Decays	15	15	Backgrounds	10	20
Total Statistical	95	105	Total Systematics	70	90

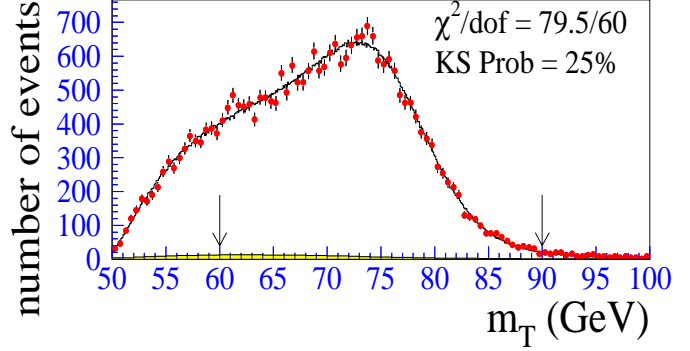
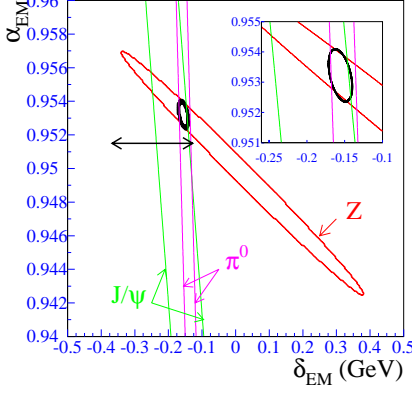


FIG. 2. The left figure shows the constraints on the DØ electromagnetic energy scale parameters from collider data. The transverse mass distribution of $W \rightarrow e\nu$ events from DØ Run IB data with the best fit superimposed is shown on the right.

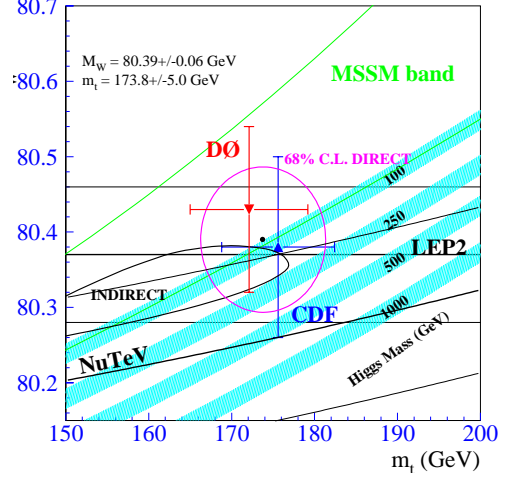
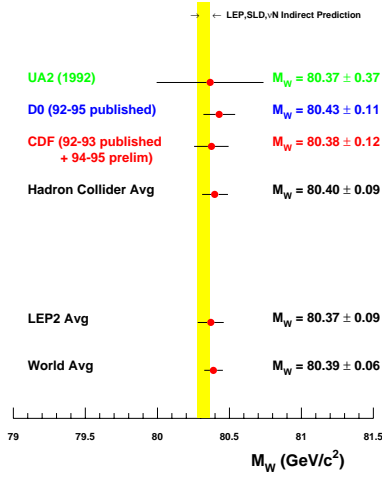


FIG. 3. A summary of direct M_W measurements is shown on the left including the world average. The right figure illustrates the constraints on the Higgs mass imposed by the present Tevatron M_W and M_t measurements as well as by the ones from LEP, NuTeV and SLC. The bands represent the prediction of the MSSM.

C. $W \rightarrow \tau\nu$ and g_τ^W/g_e^W

Both CDF and DØ have measured W production in the mode $W \rightarrow \tau\nu$ where τ decays hadronically. The signature of hadronic decay of the τ is an isolated narrow jet composed of highly boosted decay products. The event selection requires $E_T(jet) > 25$ GeV/c and $\cancel{E}_T > 25$ GeV. The signal and QCD backgrounds ($< 20\%$) are estimated using the $E_T(jets)$ profile distribution (fractional \cancel{E}_T in the two hottest towers of the τ jet). The DØ preliminary results are $\sigma \cdot BR(W \rightarrow \tau) = 2.38 \pm 0.09$ (stat) ± 0.10 (sys) ± 0.1 (lum) nb and $g_\tau^W/g_e^W = 1.004 \pm 0.032$.

The CDF collaboration having a silicon vertex detector has used the decay $\tau \rightarrow e\nu\nu$ to measure $R_{BR} = BR(W \rightarrow \tau\nu)/BR(W \rightarrow e\nu)$. The technique is based on the difference in electron impact parameter distributions in a sample of single electron events composed of $W \rightarrow e\nu$ decays, $W \rightarrow \tau\nu$, $\tau \rightarrow e\nu\nu$ decays and QCD backgrounds. A likelihood fit to the branching fraction R_{BR} is performed using $f(d_0; b, c) = af_e(d_0) + bf_\tau(d_0) + cf_{bkg}(d_0)$ where the relevant impact parameter distributions $f_e(d_0)$, $f_\tau(d_0)$ are extracted from Monte Carlo and $f_{bkg}(d_0)$ from QCD data. The results are $R_{BR} = 1.03_{-0.32}^{+0.38} \pm 0.18$ and $g_\tau^W/g_e^W = 1.01 \pm 0.17 \pm 0.09$ consistent with hadronic τ decay measurements and $\tau - e$ universality.

D. $W(p_T)$ Distribution

The CDF collaboration has measured the $p_T(W)$ distribution in the decay mode $W \rightarrow e\nu$ using Run I data ($\int \mathcal{L} dt = 110 \text{ pb}^{-1}$). The measurement goals are to test perturbative QCD at large p_T ($> 20 \text{ GeV/c}$) and differentiate gluon resummation techniques [7] (such as q-t-space vs b-space) at small p_T ($< 10 \text{ GeV/c}$). Moreover the knowledge of the W/Z production is essential for the search for new physics and is a source of systematics for the measurements of M_W , α_s , etc. The event selection demands an electron with $p_T(e) \geq 25 \text{ GeV/c}$ and $\cancel{E}_T \geq 25 \text{ GeV}$. The major backgrounds ($< 15\%$) are due to QCD electron fakes, $W \rightarrow \tau\nu \rightarrow e\nu\nu\nu$ and the one-legged decays of $Z \rightarrow ee$.

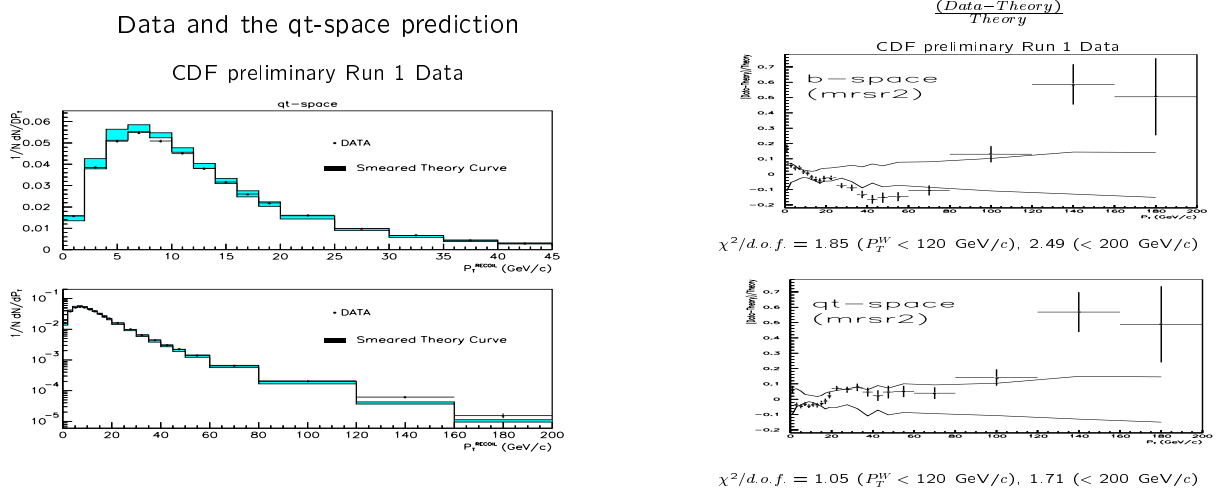


FIG. 4. The comparison of data and theoretical predictions using the qt-space gluon resummation technique for $p_T(W)$ distribution (CDF) is shown on the left. On the right, the ratio (Data-Theory)/Theory is plotted as a function of $p_T(W)$ using the qt-space and b-space gluon resummation methods.

The $p_T(W)$ distribution using qt-space gluon resummation technique is shown in Figure 4. Figure 4 also displays the ratio (data-theory)/theory vs $p_T(W)$ for both resummation techniques. The theory distributions used are obtained by adding the single boson backgrounds and are smeared with detector resolutions while the data distributions are after the subtraction of the QCD background. Both resummation techniques agree with data up to $p_T(W) \approx 120 \text{ GeV}$. At higher $p_T(W)$ region, there appears to be some discrepancy as in the case of CDF $Z \rightarrow ee$ data [8]. The recently completed $D\bar{O}$ $W(p_T)$ measurements can be found in reference [9].

III. SEARCH FOR ANOMALOUS GAUGE COUPLINGS

The effective CP conserving Lagrangian for the description of anomalous gauge couplings (AGC) is given by [10]:

$$iL_{eff}^{WWV} = g_{WWV} \{ g_1^V (W_{\mu\nu}^\dagger W^\mu - W^{\dagger\mu} W_{\mu\nu}) V^\nu + \kappa_V W_\nu^\dagger W_\nu V^{\mu\nu} + (\lambda/m_W^2) W_{\rho\mu}^\dagger W_\nu^\mu V^{\nu\rho} + ig_5^V \epsilon_{\mu\nu\rho\sigma} [(\partial^\rho W^{\dagger\mu}) W^\nu - W^{\dagger\mu} (\partial^\rho W^\nu)] V^\sigma \}$$

where $V = Z, \gamma$. If CP violating terms are allowed, three additional terms will appear in the above Lagrangian. The overall couplings are defined as $g_{WW\gamma} = e$ and $g_{WWZ} = e \cot\theta_W$. At tree level in the SM, the parameters are uniquely determined: $g_1^Z = g_1^\gamma = \kappa_Z = \kappa_\gamma = 1, \lambda_Z = \lambda_\gamma = g_5^Z = g_5^\gamma = 0$. For on-shell photons, $g_1^\gamma = 1$ and $g_5^\gamma = 0$ are fixed by electromagnetic gauge invariance while g_1^Z and g_5^Z may, however, differ from their SM values. The deviations from tree level SM values can be cast as: $\Delta g_1^Z = (g_1^Z - 1), \Delta\kappa_\gamma = (\kappa_\gamma - 1), \Delta\kappa_Z = (\kappa_Z - 1), \lambda_\gamma, \lambda_Z, g_5^Z$. Most theoretical arguments suggest that these anomalous couplings are significant at $O(m_W^2/\Lambda^2)$ where Λ is the scale of new physics. To avoid unitarity violations the coupling parameters should be expressed as form factors such as: $\lambda(\hat{s}) = \lambda/(1 + \hat{s}/\Lambda_{FF}^2)^2$; $\Delta\kappa(\hat{s}) = \Delta\kappa/(1 + \hat{s}/\Lambda_{FF}^2)^2$ with Λ_{FF} as the form factor scale. The tree level Feynman diagrams for $p\bar{p} \rightarrow WW/WZ$ production at the Tevatron are shown in Figure 5.

Limits on these couplings are usually obtained under the assumption of equal couplings for $WW\gamma$ and WWZ ($g_1^\gamma = g_1^Z = 1, \Delta\kappa_\gamma = \Delta\kappa_Z$, and $\lambda_\gamma = \lambda_Z$). In the literature, another set of relations is frequently used, the HISZ relations [11] where the WWZ and $WW\gamma$ couplings are related by: $\Delta\kappa_Z = \Delta\kappa_\gamma(1 - \tan^2 \theta_W)/2$; $\Delta g_{1Z} = \Delta\kappa_\gamma/2 \cos^2 \theta_W$; $\lambda_Z = \lambda_\gamma$.

The evidence for non SM physics contributions will be an enhancement in the high $p_T(W)$ region [12]. Figure 5 illustrates the predicted number of events in the mode $WW/WZ \rightarrow \mu\nu jj$ (for Run 1B) vs the $p_T(W)$ as a comparison of SM and non SM physics (for $\lambda = 1$ and $\Delta\kappa = 1$). Therefore, a study of the $p_T(W)$ spectrum of WW/WZ production will provide a sensitive test of the WWZ and $WW\gamma$ couplings.

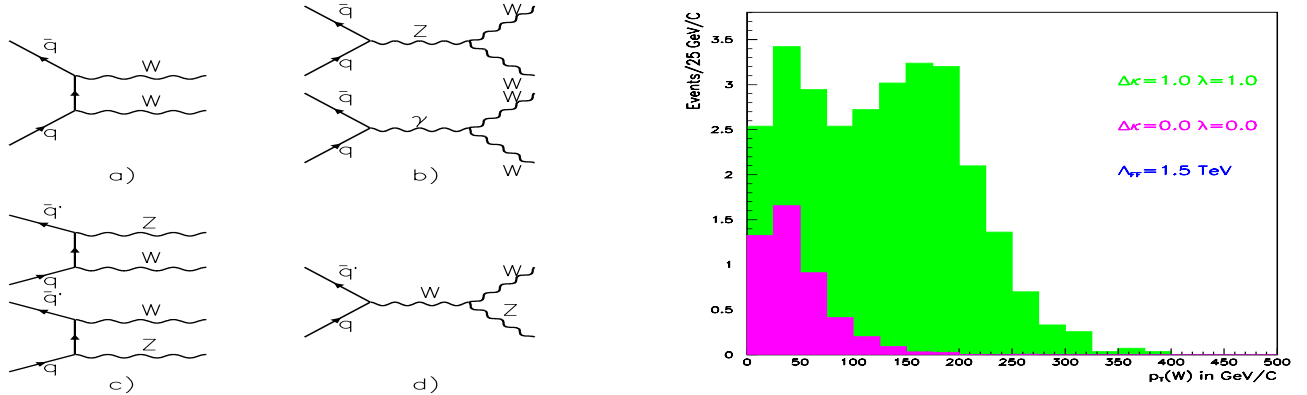


FIG. 5. The tree level Feynman diagrams for $p\bar{p} \rightarrow WW/WZ$ production at the Tevatron are shown on the left. The right figure shows the comparison of the Standard Model and Anomalous Gauge Coupling predictions for $\int \mathcal{L} dt = 80.7 \text{ pb}^{-1}$ at the DØ Run I detector in the channel $WW/WZ \rightarrow \mu\nu jj$.

A. $WW/WZ \rightarrow \mu\nu jj$

The 1994-95 data with $\int \mathcal{L} dt = 80.7 \text{ pb}^{-1}$ were used in the search for anomalous WW/WZ production in the mode $WW/WZ \rightarrow \mu\nu jj$. The event selection requires a high p_T muon ($> 20 \text{ GeV}/c$), $\cancel{E}_T > 20 \text{ GeV}$ and at least two good jets with $p_T(jet) > 20 \text{ GeV}/c$. There is no differentiation between the two processes $W \rightarrow jj$ and $Z \rightarrow jj$ due to limited mass resolution of the calorimeter. The invariant mass of the two highest E_T jets in the event is required to be between 50 and 110 GeV/c^2 along with a constraint on the transverse mass $M_T(\mu\nu) = [2 \cdot E_T^\mu \cdot \cancel{E}_T \cdot (1 - \cos(\phi_\mu - \phi_\nu))]^{1/2} > 40 \text{ GeV}/c^2$. The final event count is 224 ± 15 while the SM prediction is 4.5 ± 0.8 events.

The major sources of backgrounds are from QCD multijet and $W + \geq 2$ jet events with $W \rightarrow \mu\nu$. The QCD multijet background is due to misidentifying a muon contained in one of the jets as an isolated muon and where there is significant \cancel{E}_T . This background is estimated from data using a control sample to determine muon fake probability [13]. The $W + \geq 2$ jets contribution is computed using a Monte Carlo sample generated with VECBOS, HERWIG [14] (hadronization) and GEANT [15] for detector simulation. Normalization of this background is determined by comparing the number of expected events outside the dijet mass window after the subtraction of the QCD multijet contribution. The final background contributions are 105 ± 19 (QCD multijet), 117 ± 24 ($W + \geq 2$ jets) and 2.7 ± 1.2 (others) without systematics. The total background contribution to the final sample are $224.5 \pm 32.7 \pm 45.8$.

TABLE II. The DØ Run IB $WW/WZ \rightarrow \mu\nu jj$ axis limits (one-dimensional) at the 95% confidence limits (C.L.) with the assumption of equal $WW\gamma$ and WWZ couplings and the HISZ relations. The limits are listed for two different values of Λ_{FF} along with the relevant unitary bounds.

95% C.L. Limits	$\Lambda_{FF} = 1.5 \text{ TeV}$	Unitary Bounds	$\Lambda_{FF} = 2.0 \text{ TeV}$	Unitary Bounds
$\lambda_\gamma = \lambda_Z$ ($\Delta\kappa_\gamma = \Delta\kappa_Z = 0$)	-0.45, 0.46	-0.82, 0.82	-0.43, 0.44	-0.46, 0.46
$\Delta\kappa_\gamma = \Delta\kappa_Z$ ($\lambda_\gamma = \lambda_Z = 0$)	-0.62, 0.78	-1.17, 1.17	-0.60, 0.74	-0.66, 0.66
λ_γ (HISZ) ($\Delta\kappa_\gamma = 0$)	-0.44, 0.46	-0.82, 0.82	-0.42, 0.44	-0.46, 0.46
$\Delta\kappa_\gamma$ (HISZ) ($\lambda_\gamma = 0$)	-0.75, 0.99	-2.17, 2.17	-0.71, 0.96	-1.22, 1.22

The comparison of the final data sample and the total background as a function of $p_T(W)$ is shown in Figure 6. The data and background distributions are consistent with each other signalling no evidence of AGC. This agreement is translated into AGC limits by means of a binned maximum likelihood method with convoluting Gaussian errors for the prediction and background uncertainties. The 95% C. L. limits for the coupling parameters λ and $\Delta\kappa$ are tabulated in Table II for the cases of equal WWZ and $WW\gamma$ couplings and the HISZ relations. The contour constraining the coupling parameters in the $\lambda - \Delta\kappa$ plane is illustrated in Figure 6 for $\lambda_{WW\gamma} = \lambda_{WWZ}$ and $\Delta\kappa_{WW\gamma} = \Delta\kappa_{WWZ}$.

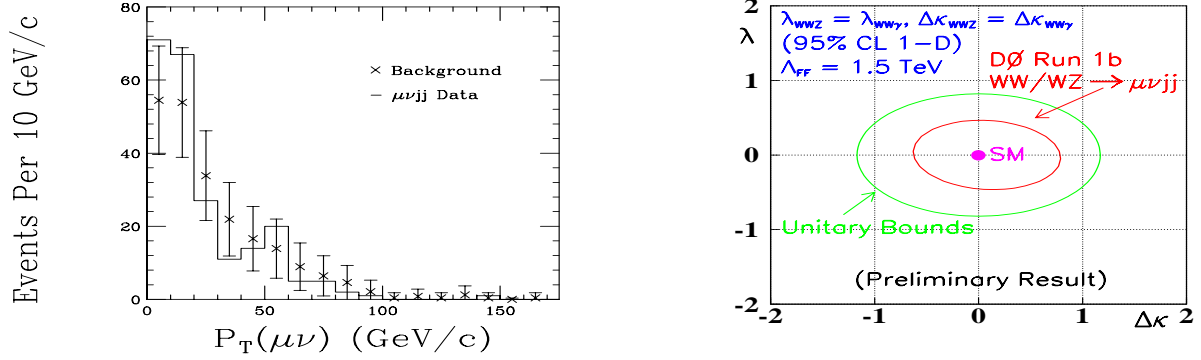


FIG. 6. Comparison of the final data sample and estimated total background as function of $p_T(W)$ for $WW/WZ \rightarrow \mu\nu jj$ is shown on the left. On the right, the contour plot of allowed region in the $\lambda - \Delta\kappa$ plane at 95% C.L. for $\Lambda = 1.5$ TeV. The outer ellipse shows the bounds imposed by the relevant unitary conditions.

B. Overview of the DØ Diboson Projects

The DØ collaboration has done a comprehensive search [16] for anomalous gauge couplings in the four diboson final states $p\bar{p} \rightarrow WW, WZ, W\gamma, Z\gamma$ in twelve different decay modes using Run I data. A detailed listing of the diboson final states and the relevant decay channels including the status of the searches is given in Table III. The limits from all different channels have been combined to produce the final AGC coupling limits from DØ in Run I.

C. Run I DØ Combined Anomalous Coupling Limits

The combined limit of $WW/WZ \rightarrow \mu\nu jj$ channel along with 11 other channels listed in Table III has been produced. This involves performing a simultaneous binned maximum likelihood fit to the observed number of events and the expected number of signal and background distributions: $p_T(\gamma)$ spectrum in the $W\gamma$ channels, $p_T(l)$ distribution in $WW \rightarrow l\nu l\nu$ modes, $p_T(W \rightarrow l\nu)$ spectrum in the $WW/WZ \rightarrow l\nu jj$ channels and to the observed number of events in the $WZ \rightarrow l\nu ee$ after a careful account of correlated and uncorrelated uncertainties in different data sets and modes. The one-dimensional 95% C.L. axis limits for the various coupling cases are given in Table IV.

TABLE III. A summary of the comprehensive search for anomalous trilinear gauge couplings by DØ using Run I data in 12 different channels.

Diboson State	Channel	Coupling	Status
$Z\gamma$	$\rightarrow ee\gamma, \mu\mu\gamma$	$Z\gamma\gamma, ZZ\gamma$	Published
	$\rightarrow \nu\nu\gamma$		'93-94 Data: published ('94-95 Data: in progress)
$W\gamma$	$\rightarrow e\nu\gamma, \mu\nu\gamma$	$WW\gamma$	Published
WW	$\rightarrow e\nu e\nu, e\nu\mu\nu, \mu\nu\mu\nu$	$WW\gamma, WWZ$	Published
WZ	$\rightarrow e\nu ee, \mu\nu ee$	WWZ	Completed
WW/WZ	$\rightarrow e\nu jj$	$WW\gamma, WWZ$	Published
	$\rightarrow \mu\nu jj$		Completed
Combined Limit	All completed	$Z\gamma\gamma, ZZ\gamma, WW\gamma, WWZ$	Completed except '94-95 $Z(\nu\nu)\gamma$

IV. SUMMARY AND OUTLOOK

The CDF and DØ collaborations have done a number of world class measurements of electroweak parameters using 1992-96 data such as $R_{e+\mu} = 10.48 \pm 0.43$, $\alpha_W = 2.126 \pm 0.092$ GeV (indirect), $M_W = 80.43 \pm 0.11$ GeV, $g_\tau^W/g_e^W = 1.004 \pm 0.032$. The diboson channels $WW/WZ \rightarrow \mu\nu jj$, $WZ \rightarrow \mu\nu ee$, $e\nu ee$ have been completed. Combined with other DØ channels previously announced, these provide some of the most stringent limits on the anomalous coupling parameters. Looking towards future, the Main Injector is close to operation. The CDF and DØ detectors are undergoing major upgrades. We expect much larger data sets with much improved detectors in Run II. Both collaborations are looking forward to an exciting Run II with many precision measurements and new discoveries.

TABLE IV. The DØ Run I combined 1-D limits at 95% C.L. from a simultaneous fit to the $W\gamma$, $WW \rightarrow$ dileptons, $WW/WZ \rightarrow e\nu jj, \mu\nu jj$, and $WZ \rightarrow$ trilepton data samples for four different relations between WWZ and $WW\gamma$ couplings.

95% C.L. Limits	$\Lambda = 1.5$ TeV	$\Lambda = 2.0$ TeV
$\lambda_\gamma = \lambda_Z$ ($\Delta\kappa_\gamma = \Delta\kappa_Z = 0$)	-0.20, 0.20	-0.18, 0.19
$\Delta\kappa_\gamma = \Delta\kappa_Z$ ($\lambda_\gamma = \lambda_Z = 0$)	-0.27, 0.42	-0.25, 0.39
λ_γ (HISZ) ($\Delta\kappa_\gamma = 0$)	-0.20, 0.20	-0.18, 0.19
$\Delta\kappa_\gamma$ (HISZ) ($\lambda_\gamma = 0$)	-0.31, 0.56	-0.29, 0.53
λ_Z (SM $WW\gamma$) ($\Delta\kappa_Z = \Delta g_1^Z = 0$)	-0.26, 0.29	-0.25, 0.27
$\Delta\kappa_Z$ (SM $WW\gamma$) ($\lambda_Z = \Delta g_1^Z = 0$)	-0.37, 0.55	-0.34, 0.51
Δg_1^Z (SM $WW\gamma$) ($\lambda_Z = \Delta\kappa_Z = 0$)	-0.46, 0.65	-0.44, 0.61
λ_γ (SM WWZ) ($\Delta\kappa_\gamma = 0$)	-0.27, 0.25	-0.25, 0.24
$\Delta\kappa_\gamma$ (SM WWZ) ($\lambda_\gamma = 0$)	-0.57, 0.74	-0.54, 0.69

V. ACKNOWLEDGEMENT

This work would not have been possible without the help of my DØ and CDF colleagues. This work is also supported in part by the U.S. Department of Energy Grant DE-FG03-94ER40837.

-
- [1] F. Abe *et al.* (CDF Collaboration), Nuc. Inst. Meth. Phys. Res. **A271**, 387 (1988).
 - [2] S. Abachi *et al.* (DØ Collaboration), Nuc. Inst. Meth. Phys. Res. **A338**, 185 (1994).
 - [3] R. Hamburg *et al.* Nucl. Phys. **B359**, 343 (1991); W. L. van Neervan and E. B. Zijlstra, Nucl. Phys. **B382**, 11 (1992).
 - [4] S. Eno for DØ Collaboration, Talk presented at the Les Rencontres de Physique de la Vallée d' Aoste, LaThuille, Italy, February 28 - March 6, 1999. The latest CDF results can be seen at <http://www-cdf.fnal.gov/physics/ewk/ewk.html>.
 - [5] S. Abachi *et al.* (DØ Collaboration), Phys. Rev. Lett. **75**, 1456 (1995).
 - [6] K. S. McFarland *et al.*, Proc. of the XXXIII Rencontre de Moriond, March 1998, Les Arcs, France.
 - [7] P. B. Arnold, R. P. Kaufman, Nucl. Phys. **B349**, 381 (1992); J. Collins, D. Soper, and G. Sterman, Nucl. Phys. **B250**, 199 (1985); R. K. Ellis and S. Veseli, Nucl. Phys. **B511**, 649 (1998); R. K. Ellis *et al.*, Nucl. Phys. **B503**, 309 (1997).
 - [8] Robert Wagner, private communication.
 - [9] M. Mostafa for DØ Collaboration, Talk presented at the APS Meeting, Atlanta, GA, March 21-26, 1999. See also at <http://www-d0.fnal.gov/public/d0-physics.v2.html>.
 - [10] K. Hagiwara, R. D. Peccei, D. Zeppenfeld, and K. Hikasa, Nucl. Phys. **B282**, 2253 (1987); K. Hagiwara, J. Woodside, and D. Zeppenfeld, Phys. Rev. **D41**, 2113 (1990).
 - [11] K. Hagiwara *et al.*, Phys. Rev. **D48**, 2182 (1993).
 - [12] K. Gaemers and G. Gounaris, Z. Phys. **C1**, 259 (1979).
 - [13] B. Abbot *et al.*, (DØ Collaboration), Phys. Rev. **D54**, 052001 (1998).
 - [14] G. Marchesini *et al.*, Phys. Comm. **67**, 465 (1992).
 - [15] F. Carminati *et al.*, GEANT Users Guide, CERN Program Library Long Writeup WSO13 91993), unpublished.
 - [16] S. Abachi *et al.*, (DØ Collaboration), Phys. Rev. Lett., **75**, 1023 (1995); Phys. Rev. Lett., **75**, 1028 (1995); Phys. Rev. Lett., **75** 1034(1995); Phys. Rev. Lett., **77**, 3303 (1996); Phys. Rev. Lett., **78**, 3634 (1997); Phys. Rev. Lett., **78**, 3640 (1997); Phys. Rev., **D56**, 6742 (1997); S. Abbott *et al.*, (DØ Collaboration), Phys. Rev. Lett., **79**, 1441 (1997); Phys. Rev., **D57** 3817 (1998); Phys. Rev., **D58**, Rapid Comm. 051101 (1998); Phys. Rev., **D58**, Rapid Comm. 31102 (1998).